

# Depths of fracture-initiating flaws and initial stages of crack propagation in glass

R. H. DOREMUS, W. A. JOHNSON

*Materials Engineering Department, Rensselaer Polytechnic Institute, Troy, New York 12181, USA*

Scanning electron micrographs of points of fracture initiation on soda-lime glass surfaces show that the initial stages of crack propagation are complex. The circular intersection of the initial crack path with the final fracture plane is not a measure of the critical flaw depth for initiation of fracture; flaw depths measured by an etching technique are more reliable. Possible explanations for the initial crack paths observed are explored.

## 1. Introduction

Flaw or cracks in the surfaces of brittle materials lead to their failure when they are subjected to tensile stresses much below the theoretical fracture stress  $\sigma_t$ . The applied stress is enhanced at the crack tip, and the failure stress  $S_f$  is given in terms of the crack depth  $c$  and the radius  $\rho$  of the crack tip [1]:

$$S_f^2 = \frac{\sigma_t^2 \rho}{4c} \quad (1)$$

Direct measurement of the depths of fracture-initiating cracks is difficult, because the cracks are very narrow. Mould and Southwick estimated the crack depths in soda-lime glass abraded by different emery papers to range from 5 to 25  $\mu\text{m}$  with the optical microscope [2]. Ohlberg *et al.* found crack depths of 0.4 to 12  $\mu\text{m}$  in soda-lime glass damaged by silicon carbide particles, using lithium-sodium ion exchange to reveal the cracks [3]. Pavelcheck and Doremus calculated crack depths in abraded soda-lime glass from strengths of etched glass and a model of the etching process [4, 5]. Depths of about 6  $\mu\text{m}$  were found for glass with an average breaking strength at  $-196^\circ\text{C}$  of about  $1.3 \times 10^8 \text{ N m}^{-2}$  (18 500 p.s.i.). Mecholsky *et al.* measured sizes of fracture-initiating flaws in a number of glasses, glass ceramics, and brittle crystalline ceramics from microscopic observation to be from 25 to 200  $\mu\text{m}$ ; they found flaws in various silicate glasses to be about 60 to 80  $\mu\text{m}$  in size [6]. From observations of the origins of frac-

tures in soda-lime glass in the scanning electron microscope, Varner and Oel found the size of the cracks initiating fracture to be about 30  $\mu\text{m}$  [7].

In this paper reasons for the differences between these different measurements are explored. Scanning electron micrographs of fracture-initiating flaws on the surface of soda-lime glass indicate that the initial stages of crack propagation may be rather complex. It is concluded that the flaw depths measured by etching are the most reliable, even though the method is indirect. The relations between crack path and stress fields are also explored.

## 2. Experimental methods

As-received rods of a commercial soda-lime glass (Kimble R-6, nominal composition 73%  $\text{SiO}_2$ , 15%  $\text{Na}_2\text{O}$ , 5%  $\text{CaO}$ , 4%  $\text{MgO}$ , 2%  $\text{Al}_2\text{O}_3$ , 1%  $\text{B}_2\text{O}_3$ ) 3 mm in diameter were cleaned with a compressed air dusting container and then broken by hand into segments about 1.5 cm long. Two thumbs and two fingers gave approximately a four-point bending stress on the rods. Fracture occurred between the fingers in the expected region of highest stress, and the eventual crack path was perpendicular to the sample surface. The broken segments were mounted for observation and the fracture surface cleaned with the compressed air. The specimens were then coated with a thin layer of gold or chromium by vacuum evaporation, and observed in an MAC-700 scanning electron microscope.

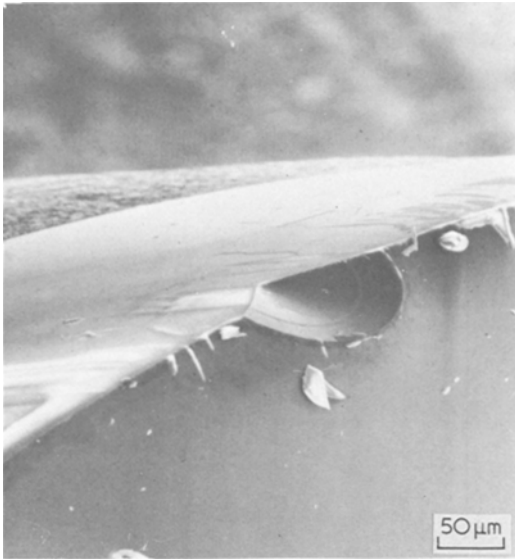


*Figure 1* Scanning electron micrograph of a fracture initiation site in soda-lime glass. Top, original glass surface, bottom, final fracture plane (mirror) (X 180).

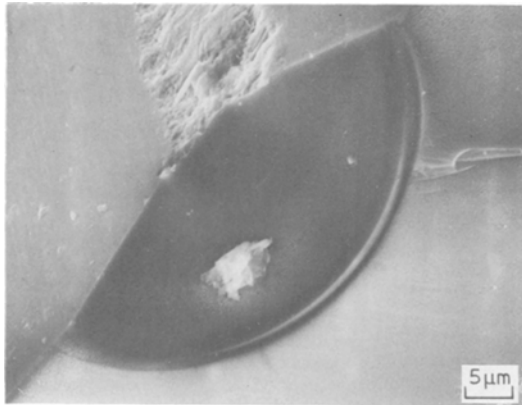


*Figure 2* Scanning electron micrograph of a fracture initiation site in soda-lime glass. Top left, original glass surface, bottom right, fracture plane (X 1200).

### 3. Experimental results

Scanning electron micrographs of the regions where cracks initiated at the glass surface are shown in Figs. 1 to 4. Figs. 3a and b and 4a and b are matched pairs from the opposite sides of the same specimen, and show that one side is a depression in the glass and the other side a protrusion. In every crack observed there was a region like those shown in Figs. 1 to 4 at the origin of the fracture mirror. Similar regions are visible in the micrographs of Varner and Oel [7].

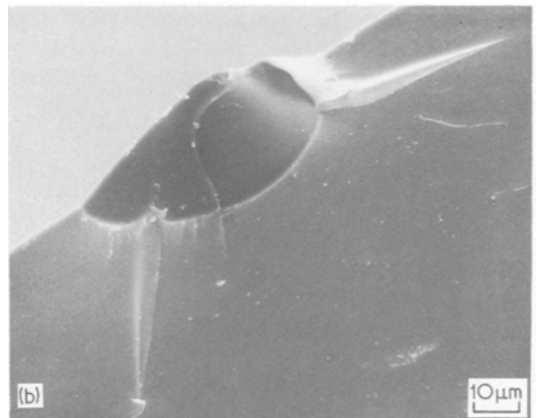
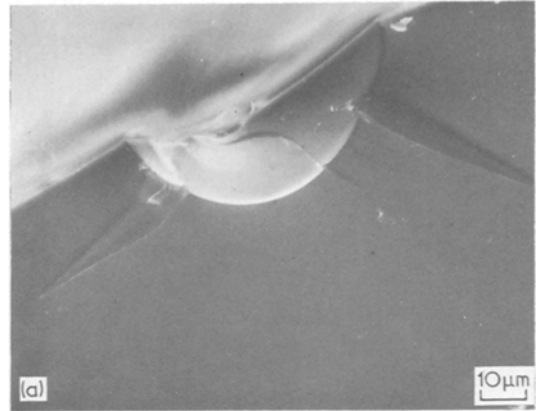


*Figure 3(a)* Scanning electron micrograph of a fracture initiation site in soda-lime glass. Top, original glass surface, bottom, fracture plane (X 610), (b) other side of (a).

### 4. Discussion

The diameters of circles intercepting the final crack plane have been taken as the depths of the crack-initiating flaw [6, 7]. However, it seems more likely that the initiating flaw was not nearly this deep, and that the spherical regions result from the early stages of crack propagation. Thus the reported [6, 7] flaw depths of greater than  $30\ \mu\text{m}$  must be regarded as not pertinent to the initiation of fracture, and the depths of about 6 to  $7\ \mu\text{m}$  for abraded soda-lime glass, as found by the etching method [4], appear to be more reasonable and in agreement with earlier approximate results [2, 3].

It is of interest to speculate on the origin and path of crack propagation that leads to the forms in Figs. 1 to 4. Consider a long, straight crack DF in the glass surface, penetrating into the glass either perpendicularly or at some angle to a depth  $c$  much less than the crack length. The crack will in

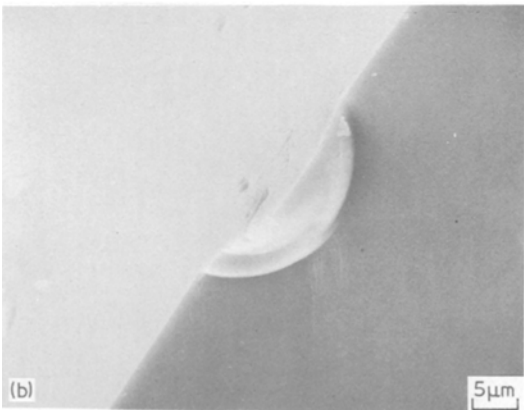
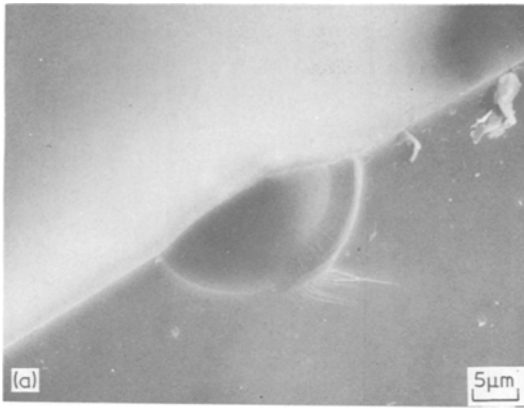


Figure 4(a) Scanning electron micrograph of a fracture initiation site in soda-lime glass. Top left, original glass surface, bottom right, fracture plane ( $\times 1220$ ). (b) other side of (a).

general be inclined to the direction of applied tensile stress, as shown in Fig. 5. The highest tensile stress on the crack tip will occur somewhere along its length, usually not at the end. When an ellipsoid of semi-axes  $a > c > b$  is subjected to tensile stress parallel to the  $b$ -axis, the highest stress occurs at the end of the  $c$ -axis [8, 9]. Such a point of highest stress at the crack tip is shown in Fig. 5 by a cross; in general it will not be at the centre of the crack, because the crack will usually be of variable depth and not a true ellipsoid.

Once fracture has started, the next step is to predict the crack path. There are substantial difficulties in explaining the crack paths shown in the figures. One might first assume that the crack would grow perpendicularly to the maximum tensile stress in the glass present before fracture. Erdogan and Sih were able to explain the extensions of straight-through cracks in glass, inclined to the directions of applied tensile stress, with this

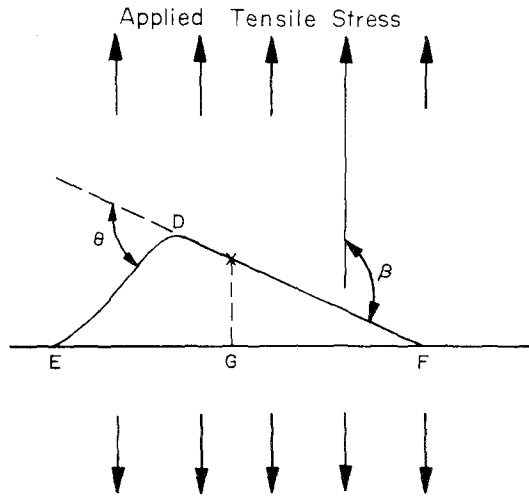


Figure 5 Schematic plane view of a crack DF in a glass surface and its propagation path DE. EGF is the final fracture plane.

assumption [10]. They found that the angle  $\theta$  (shown in Fig. 5) could be calculated from the direction of maximum tensile stress  $\sigma_\theta$  given by the plane-stress equation

$$\sigma_\theta = \frac{\cos(\theta/2)}{\sqrt{2r}} \{k_1 \cos^2(\theta/2) - \frac{3}{2} k_2 \sin \theta\} \quad (2)$$

where  $r$  is the distance from the crack tip and  $k_1$  and  $k_2$  are symmetric and skew-symmetric stress intensity factors. For example, if the applied stress is parallel to the crack,  $k_1 = 0$ , and by setting the derivative of  $\sigma_\theta$  equal to zero, the angle  $\theta$  is found to be about  $70.5^\circ$ , which was close to experimental values [9]. Thus it is possible that in the present work the crack propagated both down into the glass and along the crack length, and when it met the nearest end of the crack it changed direction by the angle  $\theta$ , determined by the angle  $\beta$  between the applied stress and the crack. This description might explain the two wings of crack propagation in the original glass surface, shown in Figs. 1 and 2. The crack paths in the glass surface in Figs. 3 and 4 are more complex, showing curvature and more than one change of direction, possibly because the initial flaw was not a single straight crack.

An explanation of the crack path into the glass is even more difficult. Solutions for the stress field around an ellipsoidal cavity have been worked out [8, 9]. However, they of course do not take into account the formation of the branch

at an angle to the original crack, which appears to influence the crack path quite strongly.

One quite important question concerns the origin of the circular trace of the initial propagation path with the final plane of fracture. A possible explanation of why the fracture occurs at this particular plane is that this plane is perpendicular to the applied stress and is defined by the equal path length X-E and X-F on the glass surface, as well as the curved path X-G down into the glass. If the crack propagates with the same velocity in all directions, the crack front will be circular when it reaches the final fracture plane E-F, and all points on the circular path will reach this plane at the same time. Then the crack abruptly changes direction and propagates with a circular path along the plane, giving the familiar mirror, mist and hackle regions on the fracture surface.

There are other interesting features shown in the micrographs. In Figs. 1, 2, and 4a, there is a rim on the initial fracture surface just before it intersects the final fracture plane. For some reason the propagating crack apparently changed direction slightly at this rim, in anticipation of the final sharp change to the fracture plane. In certain cases the circular intersection with the fracture plane was imperfect, giving rise to wing-like needles along the fracture plane (Figs. 2 and 3a and b) that were eventually smoothed out. In Fig. 3 there is a winding rim on the spherical depression, deriving from the irregular crack pattern on the glass surface.

In the above discussion no mention has been made of crack propagation caused by reaction of the crack tip with water in the atmosphere, sometimes called slow crack propagation. When glass is held under stress it becomes weaker with time.

This delayed failure or static fatigue has been explained as resulting from stress-enhanced reaction of water with the crack tip, causing the crack to deepen and sharpen [11]. Thus one might expect the very first stages of crack propagation to be related to this sort of reaction. In one second the cracks in soda-lime glass could lengthen up to tens of microns by this type of propagation. There is no evidence in the micrographs of any different mode in the early stages of propagation, so the importance of reaction-induced crack lengthening is uncertain.

This work shows that the early stages of crack propagation can be complicated, and must be taken into account in any microscopic measurement of initial flaw dimensions.

## References

1. C. E. INGLIS, *Trans. Inst. Naval Arch.* 55 (1913) 219
2. R. E. MOULD and R. D. SOUTHWICK, *J. Amer. Ceram. Soc.* 42 (1959) 582.
3. S. M. OHLBERG, L. L. SPERRY, J. M. PARSONS and H. R. GOLOB, "Advances in Glass Technology", Part 2, (Plenum Press, New York, 1962) p. 28.
4. E. K. PAVELCHECK and R. H. DOREMUS, *J. Mater. Sci.* 9, (1974) 1802.
5. *Idem*, *J. Appl. Phys.* 46 (1975) 4096.
6. J. J. MECHOLSKY, S. W. FREIMAN and R. W. RICE, *J. Mater. Sci.* 11 (1976) 1310.
7. J. R. VARNER and J. OEL, *Glastech. Ber.* 48 (1975) 73.
8. M. A. SADOWSKY and E. STERNBERG, *J. Appl. Mech., Trans. ASME* 71 (1949) 149.
9. M. K. KASSIR and G. C. SIH, *ibid* 88 (1966) 601.
10. F. ERDOGAN and G. S. SIH, *J. Basic Eng., Trans. ASME* 85 (1963) 519.
11. W. B. HILLIG and R. J. CHARLES, in "High Strength Materials", edited by V. F. Zackey, (Wiley, New York, 1965) p. 682.

Received 29 June and accepted 25 July 1977.